Pharm Res (2015) 32:3618–3635
DOI 10.1007/s11095-015-1721-3

RESEARCH PAPER

Physico-Mechanical Properties of Coprocessed Excipient MicroceLac® 100 by DM^3 Approach

Rahul V. Haware[1] • Joseph P. Kancharla[1] • Aishwarya K. Udupa[1] • Scott Staton[2] • Mali R. Gupta[1,2] • Antoine Al-Achi[1] • William C. Stagner[1]

Received: 19 February 2015 / Accepted: 19 May 2015 / Published online: 9 June 2015

ABSTRACT

Purpose To determine the effect of relative humidity (RH) and hydroxypropyl methylcellulose (HPMC) on the physico-mechanical properties of coprocessed MacroceLac® 100 using 'DM^3' approach.

Methods Effects of RH and 5% w/w HPMC on MacroceLac® 100 Compressibility Index (CI) and tablet mechanical strength (TMS) were evaluated by 'DM^3'. The 'DM^3' approach evaluates material properties by combining 'design of experiments', material's 'macroscopic' properties, 'molecular' properties, and 'multivariate analysis' tools. A 4X4 full-factorial experimental design was used to study the relationship of MacroceLac® 100 molecular properties (moisture content, dehydration, crystallization, fusion enthalpy, and moisture uptake) and macroscopic particle size and shape on CI and TMS. A physical binary mixture (PBM) of similar composition to MacroceLac® 100 was also evaluated. Multivariate analysis of variance (MANOVA), principle component analysis, and partial least squares (PLS) were used to analyze the data.

Results MANOVA CI ranking was: PBM-HPMC > PBM > MicroceLac®100 > MicroceLac®100-HPMC ($p<0.0001$). MANOVA showed PBM's and PBM-HPMC's TMS values were lower than MicroceLac®100 and MicroceLac®100-HPMC ($p<0.0001$). PLS showed that % RH, HPMC, and several molecular properties significantly affected CI and TMS.

Conclusions Significant MicroceLac®100 changes occurred with % RH exposure affecting performance attributes. HPMC physical addition did not prevent molecular or macroscopic matrix changes.

KEY WORDS coprocessed excipient · design of experiments · DM^3 · factorial design · macroscopic properties · molecular properties · multivariate analysis · multivariate analysis of variance (MANOVA) · partial least squares (PLS) · principal component analysis (PCA) · stability

List of Abbreviations

αLM	α lactose monohydrate
CI	Compressibility Index
DM^3	Design of experiment, molecular properties, macroscopic properties, and multivariate analysis
DSC	Differential scanning calorimetry
EMC	Equilibrium moisture content
ΔHd	Dehydration enthalpy
ΔHf	Fusion enthalpy
ΔHRc	Crystallization enthalpy
HPMC	Hydroxypropyl methylcellulose
MCC	Microcrystalline cellulose
MC	Moisture content
MCL	100- MicroceLac® 100
MANOVA	Multivariate analysis of variance
MUR constant	Moisture uptake rate constant
PBM	Physical binary mixture
PC	Principal component
PCA	Principal component analysis
PLS	Partial least square regression
RH	Relative humidity
TMS	Tablet mechanical strength
TGA	Thermogravimetric analysis
UMCL 100	Unexposed MicroceLac® 100. "As is MicroceLac® 100 sample", which was not exposed to any test moisture condition.
UPBM	Unexposed physical binary mixture. "As is PBM sample", which was not exposed to any test moisture condition.

✉ Rahul V. Haware
haware@campbell.edu

[1] College of Pharmacy & Health Sciences, Campbell University, Buies Creek, North Carolina 27506, USA

[2] Pharmaceutical Education & Research Center (PERC), Campbell University, Buies Creek, North Carolina 27506, USA

INTRODUCTION

Direct compression (DC) tablet manufacturing has become a 'method of choice' due to the time and cost efficiencies. DC operations exclude pretableting powder mixture treatments required in the conventional wet or dry granulations. This warrants optimized fillers and binders for successful DC tablet formulations. A variety of commercially available DC fillers and binders such as Avicel®, Emcompress®, SpheroLac 100®, and Starch 1500® have been produced by the pharmaceutical excipient industry. Ideal features expected from these DC excipients include good flowability, good compressibility, low or no moisture sensitivity, low lubricant sensitivity, and good machinability at high compression speeds with low dwell times [1]. The majority of currently available DC excipients do not possess "all the ideal and desired characteristics" required for DC formulations. For example, some of the microcrystalline cellulose grades have good powder compressibility, but poor flowability. Spray-dried lactose has acceptable flowability, but limited compressibility. Starch exhibits good disintegration, but poor flow and compressibility. Therefore, the excipient industry has designed new, high-functionality excipients to fulfill the characteristics required for DC operations [2]. These engineered excipients may reduce the drug-excipient or excipient-excipient interactions [3], need for multiple excipients, total amount of excipients required, final tablet size, and ultimately the total production cost.

Coprocessing of existing excipients is one method of producing high functionality materials that offer greater synergy than physical blending. This approach has gained wider popularity due to the high cost, timeframe, and various regulatory stages of approval associated with the discovery and development of novel excipients [4]. Excipient coprocessing involves the interaction of one excipient with another excipient at the molecular level. Coprocessing leads to changes at molecular, particle, and bulk levels [2]. The molecular level changes include the specific arrangements of molecules in a crystal lattice. This influences polymorphism, solvates or hydrates, and the development of amorphous forms. Particle level changes include particle size, shape, surface area, and porosity. Bulk level changes affected by particle assembly include flowability, compressibility, and the coprocessed excipient dilution potential [2, 5]. Since these properties are codependent, changes at one level are reflected at all other levels. Clearly, the molecular level excipient interactions modify the physical properties of the coprocessed excipient, which is not possible with simple physical dry mixing [4, 5]. Moreover, the physical properties of coprocessed excipients are modified without significant intermolecular chemical changes. The coprocessing approach achieves the synergy of improved functionality while minimizing the undesirable properties of individual excipients [1]. The United States Pharmacopeia (USP) has formally recognized this excipient class as 'coprocessed excipients' with growing interest in the development of coprocessed combinations of existing excipients. The USP has started to introduce coprocessed excipient monographs in the National Formulary [6].

Coprocessed excipients are produced by specialized manufacturing processes like spray-drying, granulation, high-shear dispersion, or melt extrusion [1, 2, 4]. These processes induce molecular level changes, which can affect the physico-mechanical properties of the developed coprocessed excipients. The spray-drying process is a good example, as it can lead to the formation of amorphous content in the coprocessed excipients [7].

Spray-drying induced amorphous content can enhance the compressibility of coprocessed excipients [7]. This has been attributed to the better plastic deformation tendency of the amorphous substances [8]. However, thermodynamically unstable amorphous content has high molecular mobility, which triggers crystallization of amorphous content into the more stable crystalline form [9, 10]. This can cause significant and unpredictable changes in the key physico-mechanical properties of the coprocessed excipients. Therefore, the coprocessed excipients might offer key challenges during handling, storing, and processing. Additionally, fundamental understanding of the coprocessed material properties is necessary to formulate pharmaceutical formulations as per "Process Analytical Technology" (PAT) guidelines issued by the United States Food and Drug Administration (US FDA) [11].

Most tablet formulations contain excipients in higher proportions than active pharmaceutical ingredients. Therefore, excipient properties can dominate formulation functionality and processability. The potential crystallization of amorphous materials associated with coprocessed excipients during handling, storing, and processing might lead to an additional source of variation in the final dosage form. During the development of a new DC formulation, the potential formulation affects of these 'new excipients' *versus* using well-characterized conventional DC excipients can be a major concern for the formulation scientist.

Konno et al. had shown the ability of hydroxypropyl methylcellulose (HPMC; Hypromellose, United States Pharmacopeia) to inhibit nucleation of solid dispersions of felodipine amorphous material in the presence of absorbed moisture by competing with crystallization promoting effects of absorbed moisture [12]. It was suggested that the stabilizing ability of HPMC at a particular concentration was based on its tendency to absorb moisture.

The purpose of the present investigation was to evaluate the effects of relative humidity (RH) and HPMC as a crystallization inhibitor on MicroceLac® 100 flow properties measured by Compressibility Index and tablet compressibility measured by tablet mechanical strength (TMS). MicroceLac® 100 is a spray-dried, coprocessed, and directly compressible excipient composed of 75% w/w of α- lactose

monohydrate (α-LM) and 25% w/w of microcrystalline cellulose. A physical binary mixture (PBM) prepared with the same composition as MicroceLac® 100 was also evaluated. The relationship of Compressibility Index (CI) and TMS with molecular properties (moisture content, dehydration, crystallization, fusion enthalpies, and moisture uptake) and macroscopic particle shape and size were evaluated by 'DM^3'. The 'DM^3' approach evaluates material properties by combining 'design of experiments', material's 'macroscopic' properties, 'molecular' properties, and 'multivariate analysis' tools. Design of experiments (DOE) provides a means to design meaningful experiments that provide the maximum amount of information from a trial. DOE also integrates statistical data interpretation and knowledge acquisition. The term multivariate analysis (MVA) is used here to include multivariate statistics such as multivariate analysis of variance (MANOVA) and multivariate data analytical techniques such as principal component analysis (PCA) and partial least squares (PLS). MVA is used to distinguish and quantify the effects of macroscopic and molecular material properties on formulation attributes. MVA allows for the analysis of multiple independent variables and dependent variables with a single experimental design. PCA and PLS can be used to mine complex associations to identify and model "hidden" phenomena that can lead to unexpected results (Fig. 1). A 4x4 full-factorial design was used in this study. The two nominal variables were excipient matrix and relative humidity, each at four levels. Multivariate analysis methods implemented in this study were multivariate analysis of variance (MANOVA), principle component analysis (PCA), and partial least square regressions (PLS). PBM and MicroceLac® 100 were exposed at 33.0%±1.9% RH, 55.0% ±2.7% RH, and 75.0%±3.0% RH following their original storage at ambient % RH (approximately 25% RH). Furthermore, the crystallization inhibitor effect of HPMC 5% w/w, on the molecular, macroscopic, and formulation properties of PBM and MicroceLac® 100 was investigated.

MATERIALS

MicroceLac® 100 (Lot no. 1243), a spray-dried, coprocessed, directly-compressible excipient, is composed of 75% w/w of αLM and 25% w/w of microcrystalline cellulose (MCC) and was a gift from Meggle Pharma, Wassenburg, Germany. SpheroLac® 100 (Lot no. 1128A4132) is αLM and was also generously donated by Meggle Pharma, Wassenburg, Germany. MCC such as Avicel® PH 102-NF (Lot no. P211823569) was donated by FMC BioPolymers, Philadelphia, PA. Compap™ L (Lot no. 099311 V567) is directly compressible acetaminophen composed of 90% w/w of acetaminophen was purchased from Covidien, Hazelwood, MO. Methocel K15M Premium [hydroxypropyl methylcellulose (HPMC)] (Lot no.YD17012N01) was purchased from the Dow Chemical Company, Midland, MI.

METHODS

Preparation of Physical Binary Mixture (PBM)

A PBM having similar composition of MicroceLac® 100 was prepared using SpheroLac® 100 (αLM) and Avicel® PH 102 (MCC). A 75% w/w of αLM and 25% w/w of MCC were blended for 10 min at 24 rpm using V-cone blender (Patterson Kelly, East Stroundsburg, PA). A second batch containing 95% w/w of PBM and 5% w/w of Compap™ L was prepared under similar blending conditions used for the PBM preparation. This was used to check the PBM blend uniformity. Compap™ L-PBM blend samples were collected from 5 different positions in the V-cone blender after blending. Samples were dissolved in methanol with vigorous mixing and adjusted to a final volume of 500 mL using distilled water. The samples (1 mL) were filtered through a polypropylene syringe filter (0.45 μ) [VWR, Radnor, PA] into a high performance liquid chromatography (HPLC) sample vials (1.8 mL). The filtrates were assayed by HPLC (HPLC-1100 Series, Agilent, Santa Clara, CA) using Luna C_{18} column (150 mm×4.6 mm internal diameter; 5 μm particle size, 100 Å pore size) from Agilent, Santa Clara, CA at 40°C column temperature. Samples were eluted under isocratic conditions. The mobile phase consisting 95% v/v water and 5% v/v acetonitrile was used at a flow rate of 1 mL/min. The sample injection volume was 5 μL. The HPLC system had a UV/Visible detector set at 243 nm wavelength. A calibration curve for acetaminophen was constructed in the range of 20 μg/mL to 100 μg/mL (r^2=0.9983).

Furthermore, PBM and MicroceLac® 100 blends were prepared with 5% w/w HPMC as per previously mentioned mixing procedure.

Molecular and Macroscopic Characterization of PBM and MicroceLac® 100

Dynamic Moisture Sorption–desorption Analysis

Dynamic moisture sorption (absorption and adsorption)–desorption analyses were performed by placing PBM, MicroceLac® 100, PBM-HPMC, and MicroceLac® 100-HPMC powders (approximately 20 mg) in a carbonized glass pan. Initially, samples were preconditioned at 25°C and 40% RH for 15 min. These samples were analyzed in triplicate using Q5000 Sorption Analyzer (TA instrument, New Castle, DE). The equilibriated PBM, MicroceLac® 100, PBM-HPMC, and MicroceLac® 100-HPMC powders were

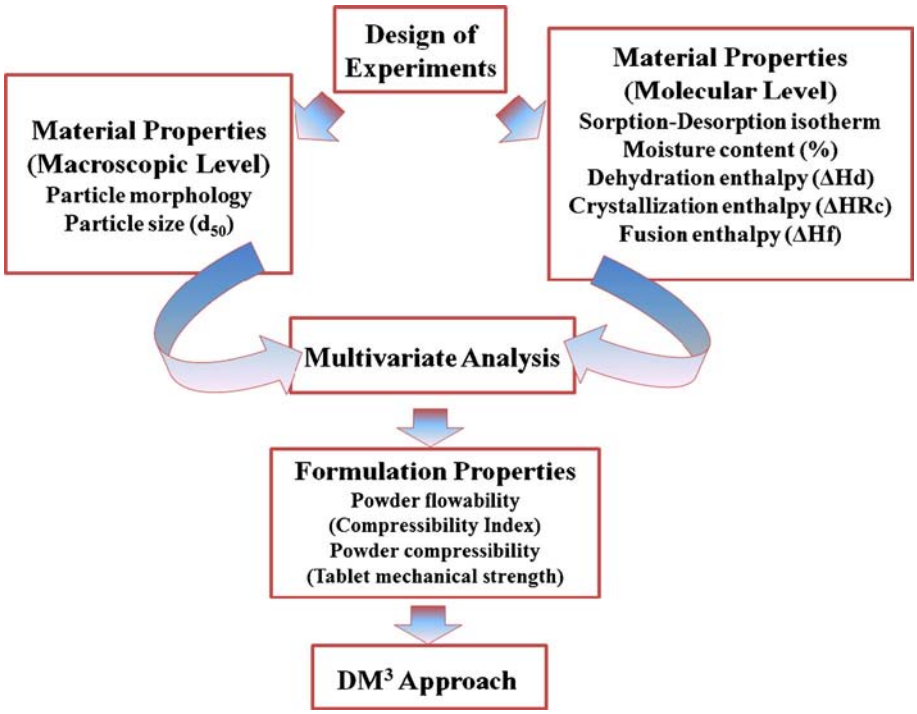

Fig. 1 Schematic representation of DM^3 approach of evaluation of material properties combing design of experiments, material's macroscopic properties, molecular properties, and multivariate analysis tools.

exposed from 0% RH to 90% RH during sorption studies, whereas desorption studies were performed by lowering % RH from 90% RH to 0% RH with step size of 10% RH and 20 min dwell time.

Static Moisture Sorption Analysis

Static moisture sorption analysis was performed by exposing PBM and MicroceLac® 100 powders at different % RH at controlled room temperature. Petri dishes containing PBM and MicroceLac® 100 powders with and without crystallization inhibitor (HPMC) were placed in separate dessicators filled with saturated solution of magnesium chloride (33.0% ±1.9% RH), magnesium phosphate pentahydrate (55.0%± 2.7% RH), and sodium chloride (75.0%±3.0% RH) for this analysis. Temperature-humidity loggers (Sper Scientific, Scottsdale, AZ) were used to measure each desiccator's % RH. Samples were monitored until equilibrium was reached. The equilibrium moisture content [EMC (%)] under static condition was calculated using Eq. 1 [13].

$$EMC(\%) = \frac{M_{water}}{M_{unexposed\ powder}} \times 100 \quad (1)$$

Where M_{water} is amount of moisture sorbed by the powder (g) and $M_{unexposed\ powder}$ is the weight of untreated PBM, MicroceLac® 100, PBM-HPMC, and MicroceLac® 100-HPMC powder (g).

Differential Scanning Calorimetry (DSC)/ Thermogravimetric Analysis (TGA)

Unexposed and exposed powders of PBM and MicroceLac® 100 with and without HPMC at different % RH were analyzed by DSC/TGA. Open pan DSC analyses were carried out using DSC Q200 (TA Instrument, New Castle, USA) without using aluminum lids. Approximately 5 mg of sample was placed in each aluminum pan. Samples were heated at 10°C /min from 25°C to 250°C. The αLM mass was corrected for the moisture content and other excipients. This corrected mass was used in the calculations of dehydration enthalpy (ΔHd), crystallization enthalpy (ΔHRc), and fusion enthalpy (ΔHf) of αLM. The moisture content correction was based on the equilibrium moisture measurements made at the various % RH. The excipient corrections were based on the percent of excipient present in a particular matrix. Furthermore, the αLM mass was corrected for HPMC, MCC, and HPMC-MCC content in PBM-HPMC, MicroceLac® 100, and MicroceLac® 100-HPMC samples respectively. These corrections allowed the enthalpy values to be based on the mass of αLM present in the matrix.

TGA measurements were carried out using TGA Q 500 (TA Instrument, New Castle, DE) with samples of approximately 20 mg weighed into each aluminum pan. Samples were heated at 10°C /min from 25°C to 180°C.

Nitrogen was used as the purge gas in both DSC and TGA analyses with flow rate of 40 mL/min and 60 mL/min

respectively. Data was analyzed using Universal Analysis software version 4.5A (TA Instrument, New Castle, DE). All DSC and TGA analyses were performed in triplicate.

Particle Size

Powder laser diffraction analyses were performed on about one gram sample in triplicate using Mastersizer® 3000 coupled with Aero S feeder (Malvern Instruments Limited, Worcestershire, UK).

Particle Morphology

The particle morphology was examined with scanning electron microscopy [SEM] (Hitachi S-3200 N, Tokyo, Japan). Samples were mounted on an aluminum base with adhesive carbon tape. Gold (60%) and palladium (40%) were used for the sample sputtering. Samples were sputtered under vacuum 10^{-4} Torr for approximately 300 s before each SEM examination.

Compressibility Index (CI)

The powder flowability was estimated by the CI. The powder CI is the percent ratio of tapped powder or particulate to the powder bulk volume. It was calculated from tapped powder and bulk densities [14]. Bulk and tapped density measurements were performed in triplicate as per the procedure described in the USP <616> using a VanKel® Tap Density Tester model 50–1200 (VanKel® Technology Group, Cary, NC) [15]. The CI ranges from less than or equal to 10 for "excellent" flowing materials to greater than 38 for very, very poor flowing materials (USP, <1174>).

Moisture Sorption Kinetics

Cylindrical, 11 mm, flat-faced tablets of PBM and MicroceLac® 100 powders with and without HPMC were prepared using a Carver Press (Carver Inc., Wabash, IN). Approximately 500.0 mg ± 1.0 mg powder was weighed and compressed at a compression pressure of 6895 kilopascals. The compressed tablets were exposed to 33.0% ± 1.9% RH, 55.0% ± 2.7% RH, and 75.0% ± 3.0% RH by keeping them on the moisture permeable sieve in the desiccator. Tablet weight was monitored at regular intervals to measure tablet moisture uptake. These experimental conditions provided an infinite source of sorbate (moisture vapor), an infinite sink of sorbent, and the planar surfaces for the penetration of moisture during the exposure period [16]. These boundary conditions give rise to a square root of time dependence of moisture uptake [17]. This relationship was used to model the moisture uptake. The square root of time relationship persists until the boundary condition assumptions are violated as saturation is approached. The moisture uptake rate (MUR) constant [$MU\ (\%)/\sqrt{t}\ (h)$] was calculated from the following Eq. 2:

$$MU = MUR\sqrt{t} \tag{2}$$

Where, MU is the percent moisture uptake.

Tablet Mechanical Strength (TMS)

Flat-faced cylindrical tablets of 11 mm diameter were prepared using the Carver Tablet Press (Wabash, IN). Approximately 500 mg of powder was manually poured into the die. Tablets of unexposed PBM and MicroceLac® 100 powders (with and without HPMC) and exposed at 33.0% ± 1.9% RH, 55.0% ± 2.7% RH, and 75.0% ± 3.0% RH were prepared. The diametrical tablet breaking force was measured by using a VanKel® Hardness Tester (Varian, Cary, NC). *TMS* was calculated according to Eq. 3 described in the USP [18].

$$TMS = \frac{2F}{\pi DH} \tag{3}$$

Where, F is the tablet breaking force in Newtons, D is the tablet diameter (mm), and H is the tablet thickness (mm).

Design of Experiments and Multivariate Analysis

A multivariate analysis of variance (MANOVA) test was used with 4x4 factorial experimental design. A statistical analysis of the data was performed using JMP Statistical Discovery Software (SAS Institute, Cary, NC). The two nominal input variables, each at four levels, were the matrix type and the relative humidity. MANOVA was performed on the formulation matrixes in order to detect differences in CI and TMS for the four different matrices. A p value of less than 0.05 was considered significant. The effect of % RH on the studied molecular and macroscopic properties of PBM and MicroceLac® 100 in the presence and absence of crystallization inhibitor (HPMC) were evaluated by PCA and PLS-1 analysis. The hidden data pattern was captured by the qualitative PCA method. The statistically significant influences of the various factors on the important powder properties like flowability (CI) and compactibility (TMS) were quantified by the PLS-1 method (The Unscrambler® 10.3, CAMO AS, Trondheim, Norway). During PLS modeling, all samples were defined as categorical variables. These categorical variables were coded as 0 and 1. The coded categorical variables were split during modeling to separate their individual influence on the response variables. Prior to PCA and PLS modeling, the design and response variables were standardized with their standard deviations in order to give each variable equal weight. Initially, a calibration model was developed on the whole data set. The uncertainty of the PLS regression

coefficients was estimated by full cross-validation and Jack-Knifing method [19]. In full cross-validation, the data were divided into two portions. A validation model was developed using all the data excluding one point, which was used to test the prediction error associated at the validation stage. This process was repeated for each data point. Finally, the validation residual variance was computed from the predicted residuals.

RESULTS AND DISCUSSION

The PBM blend uniformity containing Compap^{TM} L, αLM, and MCC was measured by evaluating acetaminophen content in the blend samples. Samples were collected from five different positions in the V-cone blender after 10 min of blending. HPLC analysis of the five collected samples showed less than 5% w/w of relative standard deviation between acetaminophen amounts in the samples. This complies with the US FDA blend uniformity guidelines [20]. Using Compap^{TM} L as a surrogate, PBM were considered to be adequately blended. Thus, αLM and MCC PBM with and without crystallization inhibitor, such as HPMC, were prepared by blending for 10 min. Likewise, MicroceLac® 100 and HPMC physical mixture was prepared under similar blending conditions.

The moisture sorption isotherm correlates the water equilibrium amount sorbed by a solid at the constant temperature and pressure. The isotherm shape, sample specific surface area, moisture uptake reversibility, and presence of hysteresis loop and its shape provide useful information about the nature of interaction between water (sorbate) and solid (sorbent) [21]. In general, high-density crystalline materials have less water

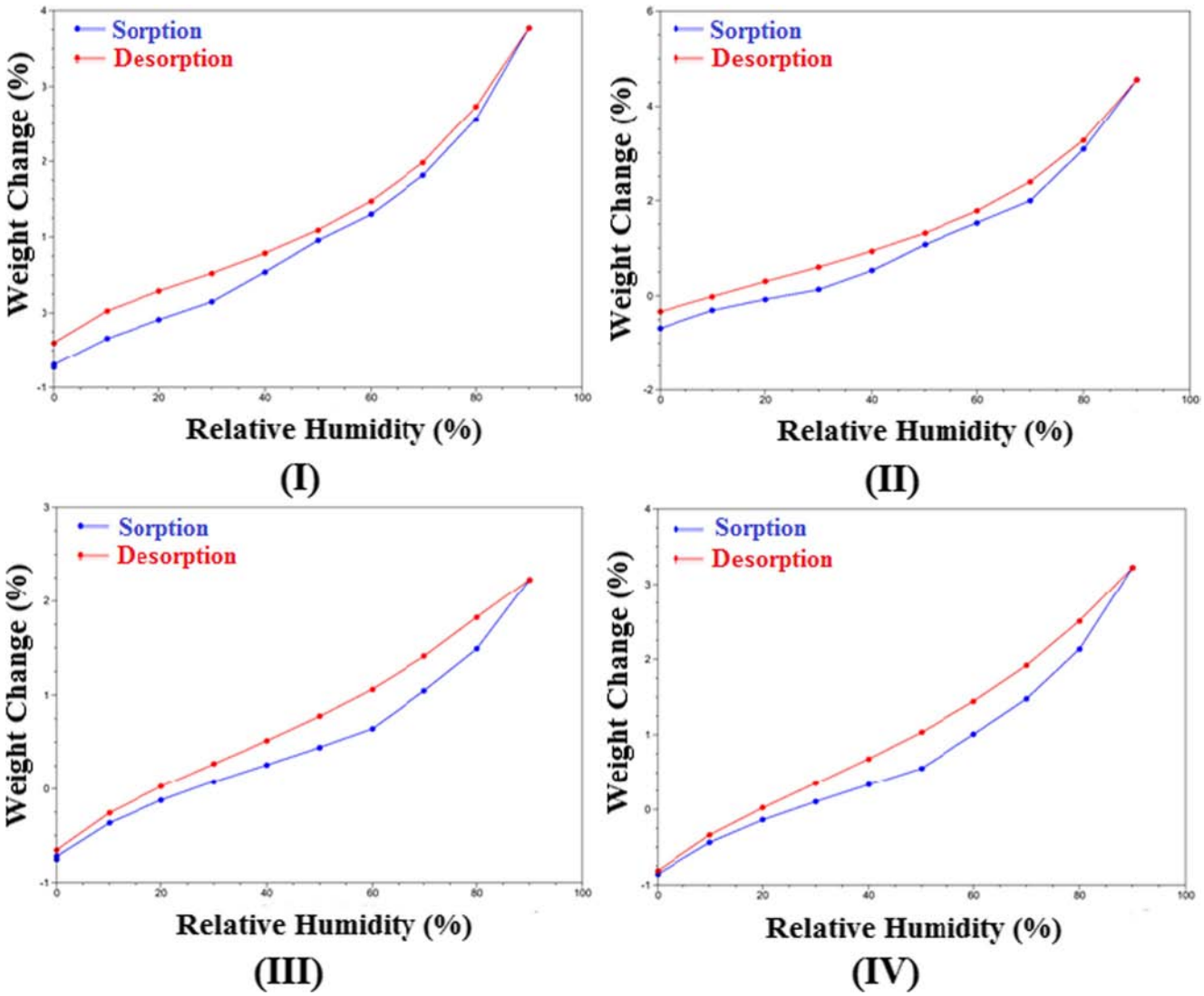

Fig. 2 Relative moisture weight change (%) of (**I**) PBM; (**II**) PBM-HPMC; (**III**) MicroceLac® 100; (**IV**) MicroceLac® 100-HPMC exposed at various percentage relative humidities [*PBM* Physical Binary Mixture, *HPMC* Hydroxypropyl methylcellulose).

affinity than porous amorphous materials. Therefore, water vapors sorb into the amorphous materials to a greater extent than simple surface adsorption like crystalline materials [12]. This leads to the greater amount of moisture sorption by amorphous solids than crystalline solids during the sorption phase. A significant amount of water sorption into the solid internal structure of amorphous materials influences the solid properties. These amorphous samples show discrepancies between the sorption and desorption isotherms at high humidities leading to hysteresis. Hysteresis indicates that the water readily condenses into mesopores (pore size of 2 to 50 μm) by capillary condensation but only desorbs from them at lower humidities than those required for condensation [22]. This phenomenon is exaggerated when material has amorphous content. Crystalline αLM shows Type III sorption isotherm with no significant hysteresis as per IUPAC nomenclature [23, 24]. Partially amorphous MCC shows sigmoidal Type II sorption isotherm with distinct "knee" at low % RH and significant hysteresis [22, 24]. The distinct "knee" is associated with the enhanced moisture adsorption at low % RH as a result of polar nature of surfaces [22]. In the present study, PBM and PBM mixed with HPMC showed Type III sorption isotherm as per IUPAC nomenclature [24]. In comparison with the αLM and MCC sorption isotherms found in the literature, PBM (Fig. 2I) and PBM-HPMC (Fig. 2II) isotherms showed greater hysteresis than crystalline αLM and lower hysteresis than partially amorphous MCC [22, 23]. PBM (Fig. 2I) and PBM-HPMC (Fig. 2II) sorption and desorption isotherms do not have the same equilibrium moisture content at 0% RH. This is most likely due to the presence of anhydrous α-lactose that converts to the monohydrate around 90% RH. The αLM is a stable hydrate and does not lose its water of crystallization at 0% RH. The PBM (Fig. 2I) and PBM-HPMC (Fig. 2II) sorption–desorption isotherms are comparable to the typical anhydrous α-lactose sorption–desorption isotherm made available by Meggle Pharma [25]. On the

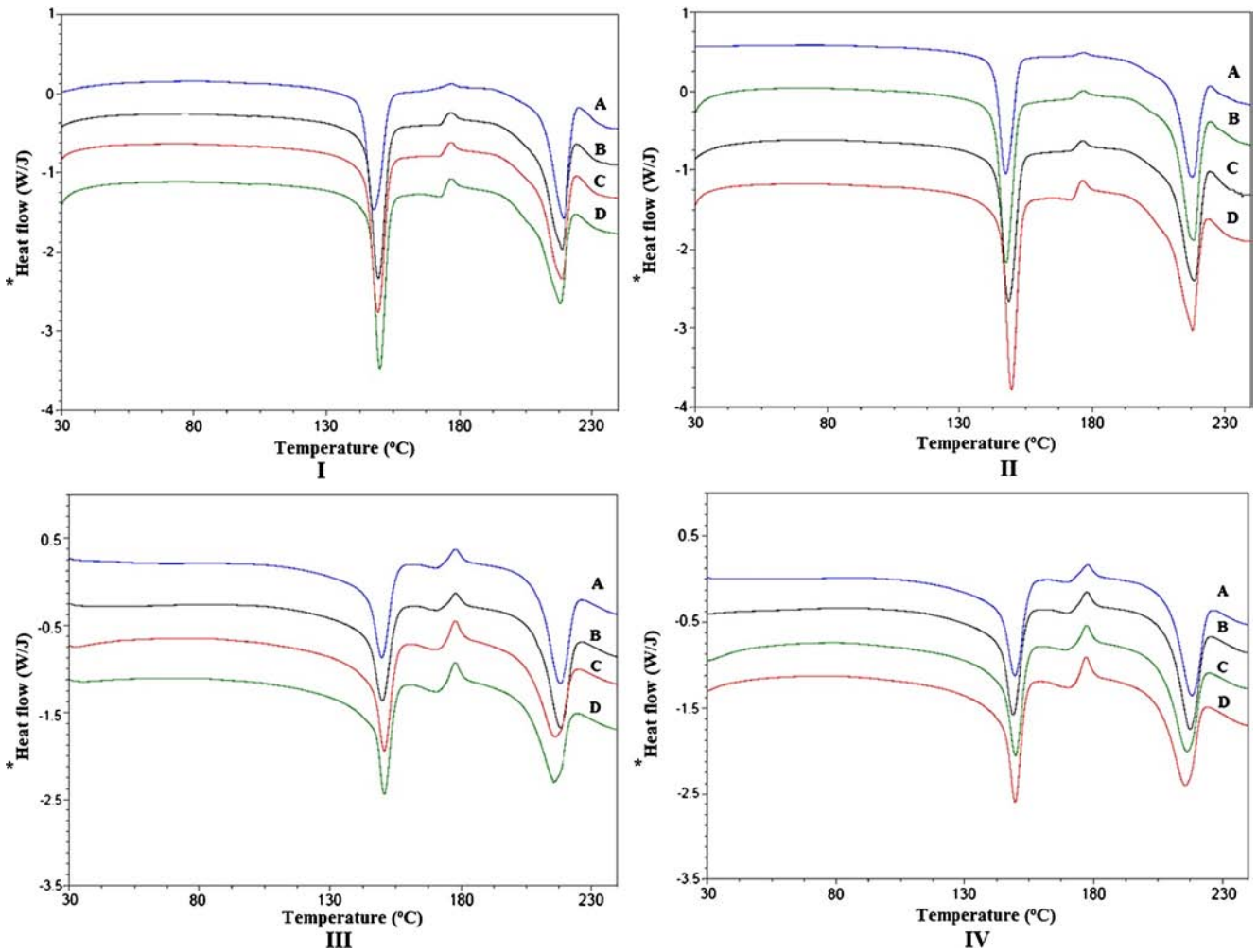

Fig. 3 Differential scanning calorimetry of (**I**) PBM; (**II**) PBM-HPMC; (**III**) MicroceLac® 100; (**IV**) MicroceLac® 100-HPMC exposed at various percentage relative humidities [*PBM* Physical Binary Mixture, *HPMC* hydroxypropyl methylcellulose; *A*- Unexposed sample; *B*-Sample exposed at 33.0% ± 1.9% RH; *C*-Sample exposed at 55.0% ± 2.7 RH; *D*- Sample exposed at 75.0% ± 3.0% RH] * Initial starting points are shifted to show the full DSC curves.

other hand, MicroceLac® 100 (Fig. 2III) and MicroceLac® 100 mixed with HPMC (Fig. 2IV) showed Type II sorption isotherm with distinct "knee" at low % RH and high hysteresis [24]. The hysteresis is likely due to a combination of the porous nature of MicroceLac® 100 (see SEM Fig. 5V) and the amorphous lactose content present in the spray-dried material. These sorption isotherms were similar to the partially amorphous MCC sorption isotherm [22]. Spray-drying induces amorphous matrix due to the rapid evaporation of saturated lactose solutions [7]. However, hysteresis of both PBM and MicroceLac® 100 isotherms in the presence and absence of HPMC seems to be Type H3 as per IUPAC nomenclature [24]. Type H3 does not exhibit any limiting adsorption and it is observed with aggregates of plate-like particles giving rise to slit-shaped pores [24].

The thermal data analysis of unexposed and exposed PBM, PBM-HPMC, MicroceLac® 100, and MicroceLac® 100-HPMC at 33.0%±1.9% RH, 55.0%±2.7% RH, and 75.0%±3.0% RH showed exothermic and endothermic events (Fig. 3). All materials showed a dehydration endotherm at 150°C, a crystallization exotherm at 174°C, and a fusion endotherm at 217°C.

The first endotherm was accompanied by the weight loss in the corresponding TGA thermograms (Fig. 4). This moisture loss is thought to be associated with αLM crystal dehydration. This is in agreement with the literature that αLM loses its water of crystallization in the range of 130°C to 170°C [26–28]. Thus, this first endothermic peak was used to measure the respective ΔHd of the samples.

Amorphous lactose showed an exothermic crystallization peak in the range of 165°C to 180°C [26, 27, 29]. This exothermic peak area was used to measure ΔHRc. Both PBM and MicroceLac® 100 showed an exothermic peak at

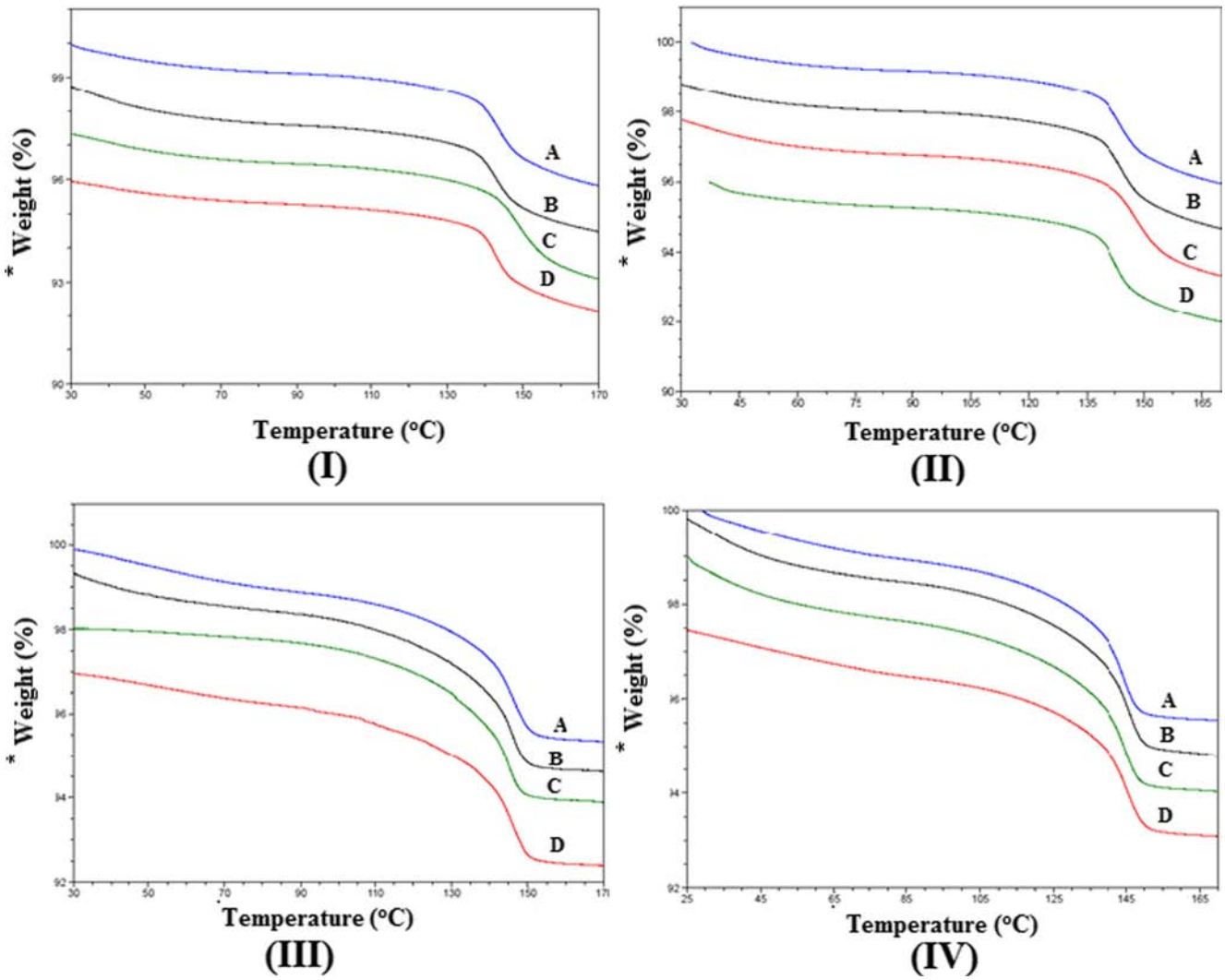

Fig. 4 Thermogravimetric analysis of (**I**) PBM; (II) PBM-HPMC; (**III**) MicroceLac® 100; (**IV**) MicroceLac® 100-HPMC exposed at various percentage relative humidities [*PBM* Physical Binary Mixture, hydroxypropyl methylcellulose; *A*- Unexposed sample; *B*-Sample exposed at 33.0% ± 1.9% RH; *C*- Sample exposed at 55.0% ± 2.7% RH; *D*- Sample exposed at 75.0% ± 3.0% RH] * Initial starting points are shifted to show the full TGA curves.

approximately 174°C. In 11 out of 12 cases, the materials exposed to increasing % RH showed higher ΔHRc values than unexposed samples. The increase in ΔHRc is also associated with an increase in MC. Water can act as a plasticizer which increases the molecular mobility of the amorphous materials [30]. The water induced material plasticization stimulates crystallization of amorphous material into the stable crystalline αLM phase during storage. The increased moisture is available to form αLM from amorphous or anhydrous lactose. During dehydration at about 150°C, the water of crystallization disrupts the crystal lattice. The water of crystallization is freed during dehydration and becomes available as water vapor to promote the crystallization of amorphous lactose present in the material. Listiohadi *et al.* proposed a similar explanation for the water vapor induced anormerization of αLM to β-lactose which was shown to occur at 177°C [27]. It is speculated that a small amount of water vapor can catalyze the transition of amorphous lactose to crystalline material resulting in an exothermic DSC peak.

The TGA thermogram did not show corresponding occurrences to the second DSC endothermic event. This second endotherm was associated with dehydrated αLM melting

Table I Measured Molecular and Macroscopic Properties of PBM and MicroceLac® 100 With and Without HPMC Exposed at Different % RH Conditions [*MC* Moisture Content (%), *ΔHd* Dehydration Enthalpy (J/g), *ΔHRc* Crystallization Enthalpy (J/g), *ΔHf* Fusion Enthalpy (J/g), *MUR* Moisture Uptake Rate Constant (% w/w/√h), d_{50} Particle Size (μm), *CI* Compressibility Index, *TMS* Tablet Mechanical Strength (MPa), *UPBM* Unexposed Physical Binary Mixture, *PBM* Physical Binary Mixture, *HPMC* Hydroxypropyl Methylcellulose, *UMCL 100* Unexposed MicroceLac® 100, *MCL 100* MicroceLac® 100]]

Sample type	MC** (%)	ΔHd* (J/g)	ΔHRc* (J/g)	ΔHf* (J/g)	MUR (% w/w/√h)	d_{50} (μm)	CI	TMS (MPa)
UPBM	2.72 (0.18)	112.88 (1.96)	1.82 (0.25)	135.20 (1.96)	0	121.0 (1.0)	22.03 (0.99)	0.030 (0.001)
PBM @33%RH	3.59 (0.07)	112.99 (6.93)	5.34 (0.38)	134.58 (6.93)	0.040 (0.010)	125.0 (3.0)	27.16 (0.15)	0.050 (0.010)
PBM @55%RH	3.90 (0.10)	112.52 (3.19)	4.81 (0.26)	143.80 (3.19)	0.200 (0.020)	116.0 (2.0)	27.50 (0.03)	0.040 (0.010)
PBM @75%RH	3.86 (0.05)	124.84 (5.17)	5.08 (0.98)	132.55 (5.17)	0.420 (0.040)	120.0 (1.0)	29.13 (0.17)	0.040 (0.010)
UPBM:HPMC	3.23 (0.63)	122.50 (1.22)	1.60 (0.42)	129.21 (1.22)	0	117.0 (1.0)	25.99 (0.09)	0.030 (0.001)
PBM:HPMC @33%RH	3.57 (0.05)	120.81 (5.34)	2.90 (0.33)	135.77 (5.34)	0.090 (0.030)	119.0 (1.0)	26.08 (1.00)	0.030 (0. 010)
PBM:HPMC @55%RH	3.63 (0.07)	127.11 (0.99)	3.63 (0.43)	142.84 (0.99)	0.370 (0.260)	119.0 (3)	30.10 (0.08)	0.040 (0.010)
PBM:HPMC @75%RH	3.75 (0.08)	129.17 (2.74)	6.16 (0.48)	137.77 (2.74)	0.580 (0.150)	122.0 (2.0)	28.43 (0.01)	0.030 (0.001)
UMCL100	4.08 (0.26)	119.70 (0.76)	7.47 (0.46)	111.90 (0.76)	0	117.0 (0.6)	22.45 (1.52)	0.076 (0.004)
MCL100 @33%RH	4.62 (0.02)	124.27 (1.93)	7.45 (0.45)	115.77 (1.93)	0.026 (0.025)	125.0 (5.0)	20.76 (0.85)	0.071 (0.004)
MCL100 @55%RH	4.83 (0.13)	130.44 (3.19)	10.45 (0.58)	119.37 (3.19)	0.155 (0.028)	134.0 (2.8)	21.88 (1.07)	0.065 (0.007)
MCL100 @75%RH	4.94 (0.18)	133.71 (1.66)	10.83 (0.43)	120.31 (1.66)	0.164 (0.001)	135.0 (5.7)	23.21 (0.22)	0.061 (0.010)
UMCL100:HPMC	4.35 (0.02)	124.22 (5.79)	7.74 (0.48)	112.62 (5.79)	0	110.0 (4.4)	15.24 (0.74)	0.085 (0.001)
MCL100:HPMC @33%RH	4.54 (0.12)	119.83 (1.92)	8.10 (0.33)	111.27 (1.92)	0.013 (0.025)	123.0 (3.0)	16.39 (0.37)	0.058 (0.005)
MCL100:HPMC @55%RH	4.83 (0.37)	127.99 (4.21)	9.49 (1.34)	115.13 (4.21)	0.189 (0.080)	124.0 (2.6)	18.79 (0.46)	0.063 (0.003)
MCL100:HPMC @75%RH	4.98 (0.02)	129.98 (1.60)	10.34 (0.40)	122.99 (1.60)	0.209 (0.000)	129.0 (8.5)	20.44 (0.53)	0.061 (0.002)

Results were derived from three measurements

All values in the parentheses indicate standard deviation

*Values were corrected for αLM amounts

** MC measured by TGA

[27–29]. This endotherm was used to measure respective fusion enthalpies (ΔHf) of the samples.

The macroscopic properties like particle size and particle morphology of PBM, PBM-HPMC, MicroceLac® 100, and MicroceLac® 100-HPMC exposed at different % RH were measured. The d_{50} values of unexposed PBM and MicroceLac®100 (Table I) were 121.0 μm and 117.0 μm respectively. These values indicated relatively close PBM and

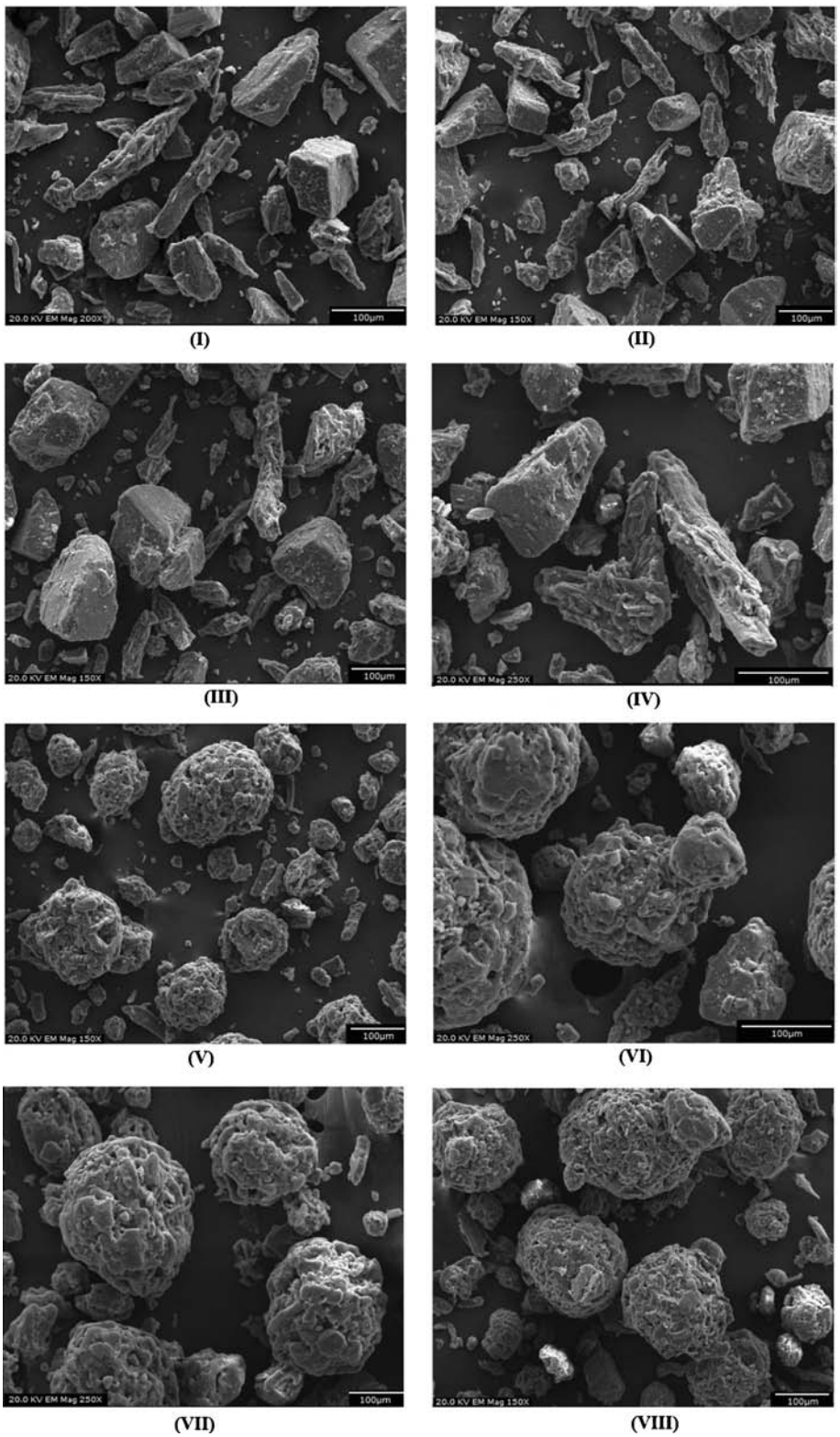

Fig. 5 Scanning electron microscopy micrographs of (**I**) Unexposed PBM (**II**) PBM exposed at 33.0 ± 1.9% RH; (**III**) PBM exposed at 55.0 ± 2.7% RH; (**IV**) PBM exposed at 75.0 ± 3.0% RH (**V**) Unexposed MicroceLac® 100; (VI) MicroceLac® 100 exposed at 33.0% ± 1.9% RH; (**VII**) MicroceLac® 100 exposed at 55.0% ± 2.7% RH; (**VIII**) MicroceLac® 100 exposed at 75.0% ± 3.0% RH [*PBM* Physical Binary Mixture].

MicroceLac®100 particle sizes. The SEM studies (Fig. 5) were carried out to evaluate the effect of % RH on the particle shape, as well as surface characteristics of PBM (Fig. 5I, II, III and IV) and MicroceLac®100 (Fig. 5V, VI, VII and VIII). The PBM SEM micrographs exhibited cube shaped αLM and fibrous MCC particles [31]. On the other hand, spray-dried MicroceLac®100 particles were composed of spherical and porous microagglomerates. The PBM and MicroceLac®100 exposure at 33.0%±1.9% RH, 55.0%±2.7% RH, and 75.0%±3.0% RH did not show change in the particle morphology.

The MANOVA analysis was performed on the formulation parameters, CI and TMS. The CI values statistically ranked in the following descending order: PBM-HPMC > PBM > MicroceLac®100 > MicroceLac®100-HPMC ($p<0.0001$). Statistically, the addition of HPMC adversely

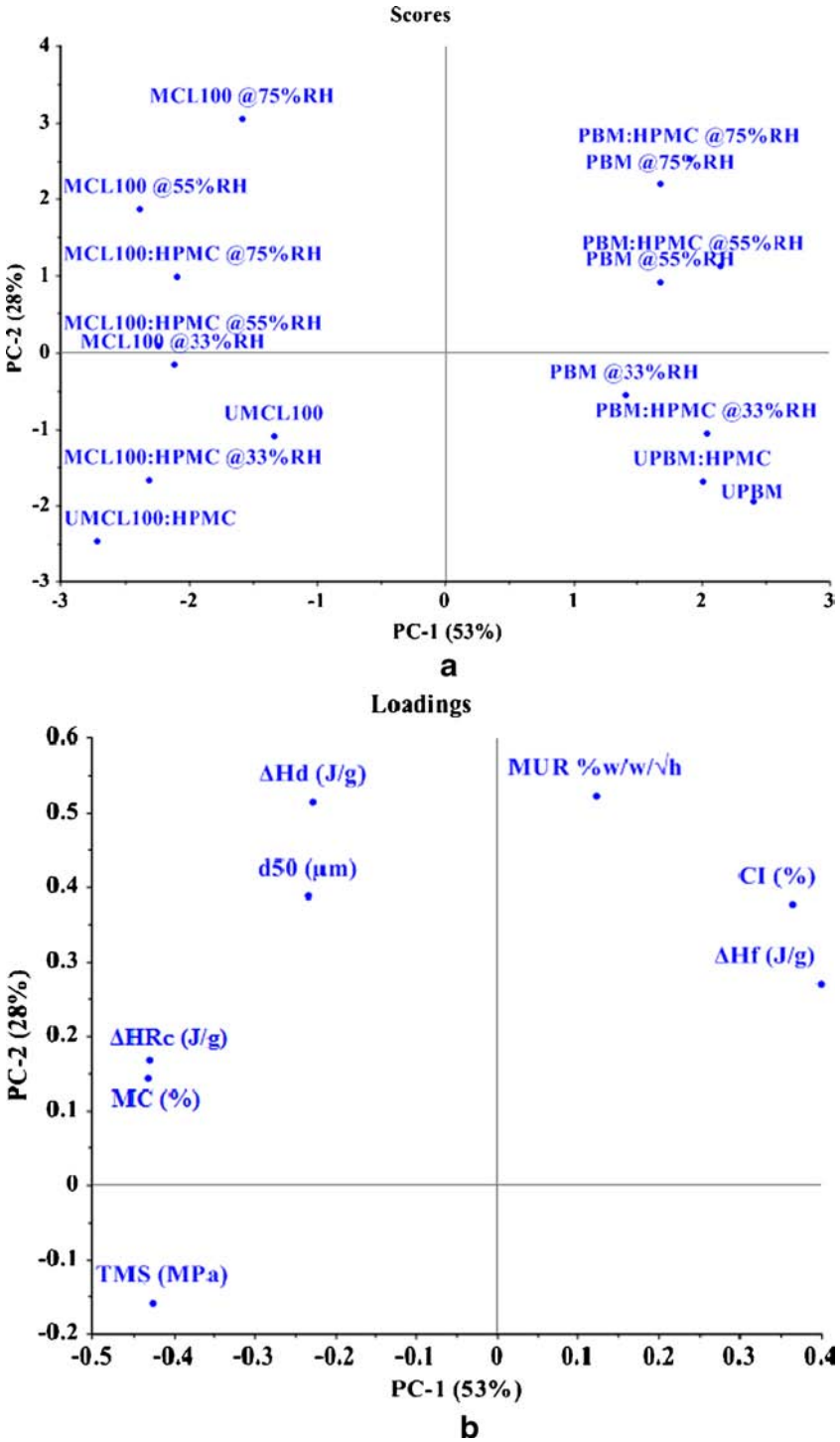

Fig. 6 **a** Principal Component Analysis (PCA) score plot of molecular properties, macroscopic properties, Compressibility Index, and tablet mechanical strength of MicroceLac® 100 and PBM unexposed and exposed at 33.0%± 1.9% RH, 55.0%±2.7% RH, and 75.0%±3.0% RH with and without HPMC. PC1 and PC2 explained 81% of the variation in the data. [*HPMC* Hydroxypropyl methylcellulose, *MCL 100* MicroceLac® 100, *PBM* Physical Binary Mixture, *UPBM* Unexposed Physical Binary Mixture, *UMCL 100* Unexposed MicroceLac® 100]. The PCA score plots were calculated from average values of measured molecular and macroscopic properties of the materials. **b** Principal Component Analysis (PCA) loadings plot of molecular properties, macroscopic properties, Compressibility Index, and tablet mechanical strength of MicroceLac® 100 and PBM unexposed and exposed at 33.0%± 1.9% RH, 55.0%±2.7% RH, and 75.0%±3.0% RH with and without HPMC. PC1 and PC2 explained 81% of the variation in the data.[*CI- CI*; *ΔHd* Dehydration enthalpy (J/g), d_{50} Particle size (μm), *ΔHf* Fusion enthalpy (J/g), *ΔHRc* Crystallization enthalpy (J/g), *MC* Moisture content (%), *MUR* Moisture uptake rate (% w/w/√h), *TMS*Tablet mechanical strength (MPa)]. The PCA loadings plots were calculated from average values of measured molecular and macroscopic properties of the materials.

affected the flow of the PBM and enhanced the flowability of MicroceLac®100. The TMS of PBM and PBM-HPMC was statistically lower than MicroceLac®100 and MicroceLac®100-HPMC ($p < 0.0001$). The coprocessed MicroceLac®100 does provide added benefit of improved TMS compared to the physical blend and supports the commercial supplier's contention that the coprocessed material provides a tableting advantage compared to the physical mixture.

A PCA of all molecular, macroscopic, and formulation properties (CI and TMS) was used to distinguish and separate data trends qualitatively (Figure 6a and b). The sample patterns and groupings were determined with a score plot (Fig. 6a). A loading plot (Fig. 6b) was employed to detect the variables that are responsible for groupings shown in the PCA score plot. Furthermore, the loading plot provides valuable information about the most critical variables as well as direct and inverse relationships between the variables. The PCA analysis details can be found elsewhere [32].

In the present study, the model uses four principal components to explain 94% of the variation in the total data matrix. Out of these four principal components, the first two principal components explained 81% of the variation in the data (Figure 6a and b). The PCA score plot (Fig. 6a) shows two distinct groupings represented along PC1. A group of PBM and PBM-HPMC is oppositely placed to the group of MicroceLac®100 and MicroceLac®100-HPMC along PC1 suggesting that the physical mixtures behave differently than the coprocessed materials. This supports the contention of the commercial supplier that the coprocessed material is not equivalent to a physical mixture. The PCA loading plot (Fig. 6b) indicates which factors are responsible for grouping in the PCA score plot. Thus, it is necessary to analyze both the PCA score and loading plot together to understand various qualitative relationships. For example, PBM (score plot, Fig. 6a) is on the positive side of PC1 origin as is ΔHf (loading plot, Fig. 6b). Therefore, these variables are directly correlated. On the other hand, MicroceLac®100 (score plot, Fig. 6a) is on the negative side of PC1 origin, while ΔHf (loading plot, Fig. 6b) is on the positive side of PC1 origin. Thus, these variables are inversely correlated. This is consistent with the expectations that substantially crystalline PBM required higher energy for melting (ΔHf). Conversely, higher amorphous MicroceLac®100 required lower energy per gram for melting. MUR constant (loading plot, Fig. 6b), MicroceLac®100, MicroceLac®100-HPMC, and PBM-HPMC (score plot, Fig. 6a) exposed at 55% RH and 75% RH, and PBM exposed at 75% RH showed direct correlation along the positive side of PC2 axis. However, in upper right positive PC1-PC2 quadrant, PBM samples with HPMC were found to have higher MUR constants than PBM samples without HPMC in this region. This can be due to the increased moisture uptake by polymer [12]. Furthermore,

Fig. 7 Partial least square (PLS) regression-1 analysis of Compressibility Index [CI] (**a**) Weighted regression coefficients of PBM and MicroceLac® 100 CI; (**b**) Weighted regression coefficients of PBM-HPMC and MicroceLac® 100-HPMC CI. These materials are exposed at different % RH (33.0% ± 1.9% RH, 55.0% ± 2.7% RH, and 75.0% ± 3.0 RH). The significance of regression is determined by full cross-validation and Martens uncertainty test and corresponds to approximately $p < 0.05$. The magnitude and sign of the coefficient's bar indicates the impact on CI. Variables with uncertainty limits that cross the zero line are statistically insignificant variables. The positive impact on CI indicate high CI value, while the negative impact on CI indicates low CI value. A high CI value means poor flowability and vice-a-versa. [*UPBM* Unexposed Physical Binary Mixture, *PBM* Physical Binary Mixture, *HPMC* Hydroxypropyl methylcellulose, *UMCL 100*- Unexposed MicroceLac® 100; MCL 100- MicroceLac® 100; MC- Moisture content (%); ΔHd- Dehydration enthalpy (J/g); ΔHf- Fusion enthalpy (J/g); ΔHRc- Crystallization enthalpy (J/g); HPMC- Hydroxypropyl methylcellulose; MUR- Moisture uptake rate (% w/w/√h); d_{50}- Particle size (μm)]. PLS models are calculated from triplicate values of measured molecular and macroscopic properties of the materials.

MicroceLac®100 and MicroceLac®100-HPMC (score plot, Fig. 6a) are positively correlated to ΔHd, ΔHRc, MC, and TMS (loading plot, Fig. 6b) in the upper left hand corner of the score and loading plot (negative side of PC1 and positive side of PC2). This suggests that less crystalline MicroceLac®100 and MicroceLac®100-HPMC sorbs moisture after exposure to 55% RH and 75% RH and interacts at the molecular level to induce crystallization of amorphous MicroceLac®100 and MicroceLac®100-HPMC content resulting in high ΔHRc. It is presumed that the crystallization process leads to the conversion of the αLM. This is associated with high ΔHd, supported by its position in upper left hand quadrant of PC1 and PC2 (Fig. 6b). From the loading plot, it can be seen that particle size (d_{50}) and CI are oppositely correlated along PC1 (Fig. 6b). It is known that increased particle size improves the powder flowability [that is low CI] [14].

The quantitative relationships between evaluated molecular and macroscopic properties of the PBM, PBM-HPMC, MicroceLac®100, and MicroceLac®100-HPMC exposed at the different % RH (X-variables) and their impact on important formulation properties like flowability (CI) and TMS (Y-variables) was established by PLS analysis. Separate PLS-1 models were performed on PBM and MicroceLac®100 with and without HPMC. These models were optimized for each Y-variable: CI and TMS (Figs. 7 and 8). The 95% confidence interval bars in Figs. 7 and 8 can be used to determine which model variables are significant. The 95% confidence interval bars of the significant coefficients do not cross the zero line. The magnitude of coefficient's bar indicates its impact on the Y-variable. Statistically insignificant design variables, interaction effects, and square effects of the main design variables were taken out during model optimization to improve model accuracy. The model accuracy was observed with regards to improvement in r^2 values and root means square at calibration and validation state values. The statistical significance of the

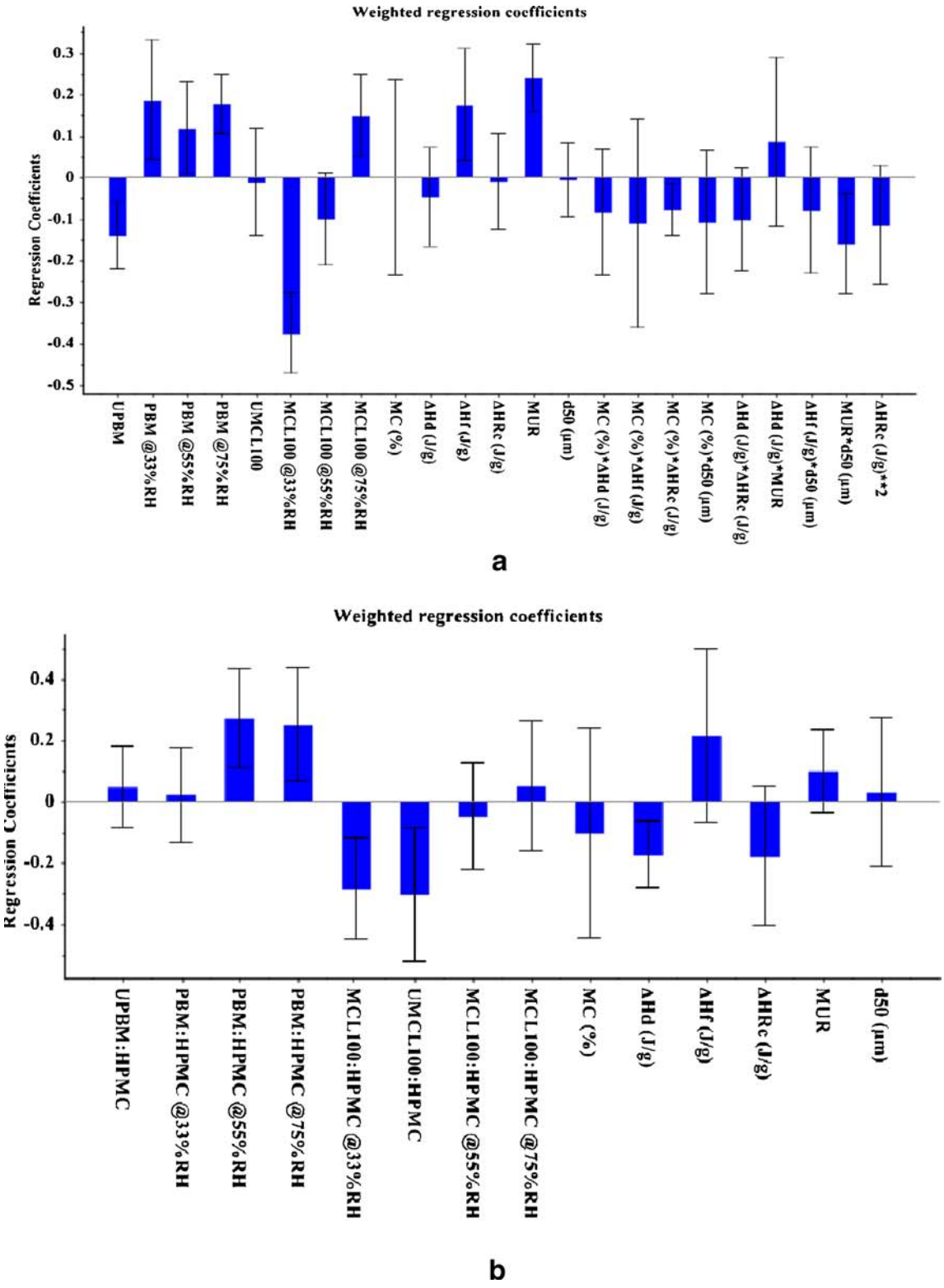

regression coefficients was determined at $p<0.05$. The optimized PLS-1 model details are given in the Table II.

The CI PLS-1 models for PBM and MicroceLac®100 with and without HPMC are shown in Fig. 7. In these models, the magnitude and sign of the coefficient's bar indicates the impact on Y-variable or response variable such as CI. Variables with uncertainty limits that cross the zero line are statistically insignificant variables. The positive impact on CI indicates high CI

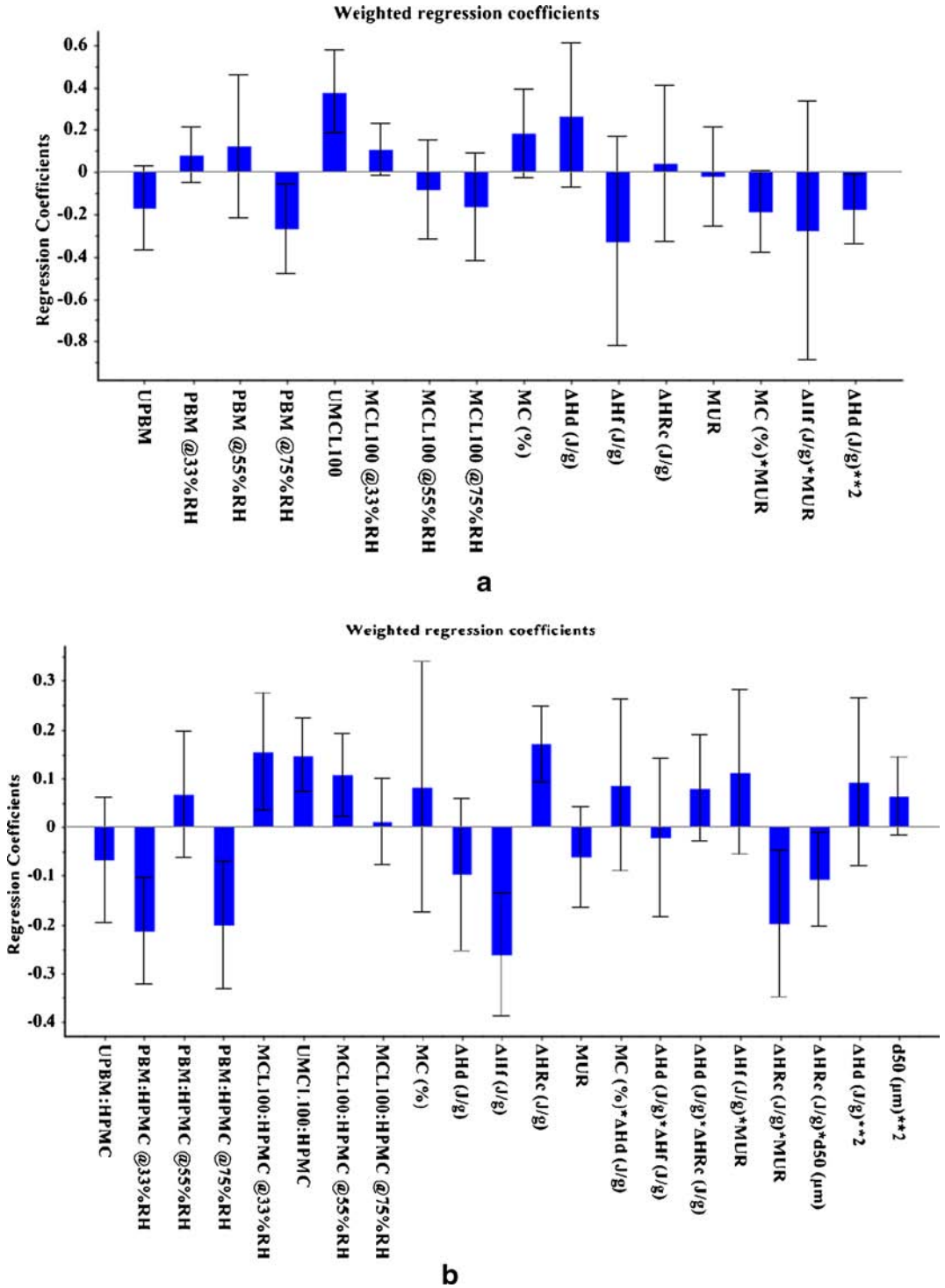

Fig. 8 Partial least square (PLS) regression-1 analysis of tablet mechanical strength [TMS (MPa)] (**a**) Weighted regression coefficients of PBM and MicroceLac® 100 TMS; (**b**) Weighted regression coefficients of PBM-HPMC and MicroceLac® 100-HPMC TMS. These materials are exposed at different % RH conditions containing HPMC (33.0% ± 1.9% RH, 55.0% ± 2.7% RH, and 75.0 ± 3.0% RH). The significance of regression is determined by full cross-validation and Martens uncertainty test and corresponds to approximately $p < 0.05$. The magnitude and sign of the coefficient's bar indicate the impact on TMS. Variables with uncertainty limits that cross the zero line are statistically insignificant variables. The positive impact on TMS indicates high TMS value, while the negative impact on TMS indicates low TMS value. A high TMS value means stronger tablets and vice-a-versa. [*UPBM* Unexposed Physical Binary Mixture, *PBM* Physical Binary Mixture, *UMCL 100* Unexposed MicroceLac® 100, *MCL 100* MicroceLac® 100, *MC* Moisture content (%), *ΔHd* Dehydration enthalpy (J/g), *ΔHf* Fusion enthalpy (J/g), *ΔHRc* Crystallization enthalpy (J/g), *HPMC* Hydroxypropyl methylcellulose, *MUR* Moisture uptake rate (% w/w/√h); d_{50}- Particle size (μm)]. PLS models are calculated from triplicate values of measured molecular and macroscopic properties of the materials.

value, while the negative impact on CI indicates low CI value. A high CI value means material shows poor flowability and vice-a-versa. The CI PLS-1 model for PBM and MicroceLac®100 without HPMC (Fig. 7a; Table II) showed that unexposed PBM, 33% RH, 55% RH, and 75% RH have significant impact on the CI. Unexposed PBM has a positive impact on the flowability, while exposure to humidity decreased the flowability. MicroceLac®100 exposed at 33% RH and 75% RH showed a respective positive and negative impact on the flowability. Though unexposed MicroceLac®100 and exposed at 55% RH showed statistically insignificant impact on the flowability, general trend of regression coefficients indicated that the exposure of

Table II Regression Coefficients of the Design Variables, Their Interactions and Square Effects, and Their Effects on the Response Variables: Compressibility Index- [CI] and Tablet Mechanical Strength [TMS (MPa)] [A: PBM:MicroceLac® 100; B: PBM-HPMC:MicroceLac® 100-HPMC; [*UPBM* Unexposed Physical Binary Mixture, *PBM* Physical Binary Mixture, *HPMC* Hydroxypropyl Methylcellulose, *UMCL 100* Unexposed MicroceLac® 100, *MCL 100* MicroceLac® 100, *MC* Moisture content (%), *ΔHd* Dehydration Enthalpy (J/g); ΔHf- Fusion Enthalpy (J/g), *ΔHRc* Crystallization Enthalpy (J/g); d_{50}- Particle Sze (μm), *MUR* Moisture Uptake Rate Constant (% w/w/√h)]]

X-variables	Y-variables			
	CI		TMS (MPa)	
	A	B	A	B
UPBM	−1.2814	X	–	X
PBM @33%RH	1.7028	X	–	X
PBM @55%RH	1.0733	X	–	X
PBM @75%RH	1.6159	X	−0.0132	X
UPBM:HPMC	X	–	X	–
PBM:HPMC @33%RH	X	–	X	−0.0121
PBM:HPMC @55%RH	X	4.3643	X	–
PBM:HPMC @75%RH	X	4.0361	X	−0.0114
UMCL100	–	X	0.0187	X
MCL100 @33%RH	−3.4492	X	–	X
MCL100 @55%RH	–	X	–	X
MCL100 @75%RH	1.3596	X	–	X
UMCL100:HPMC	X	−4.9066	X	0.0083
MCL100:HPMC @33%RH	X	−4.5798	X	0.0087
MCL100:HPMC @55%RH	X	–	X	0.0060
MCL100:HPMC @75%RH	X	–	X	–
MC	–	–	–	–
ΔHd	–	−0.1974	–	–
ΔHf	0.0478	–	–	−0.0040
ΔHRc	–	–	–	0.0010
d_{50}	–	–	–	–
MUR	5.4033	–	–	
MUR*d50	−1.2749	–	–	
MC*ΔHRc	−0.2197	–	–	
MC*MUR	–	–	−0.0046	
ΔHRc*MUR				−0.0047
ΔHRc*d50				−0.0025
ΔHd**2	–	–	−0.0019	–
B_0	6.6610	6.8611	2.3295	7.01264
Optimum no. of PCs used	5	4	5	4
Explained X-variance (%)	76	63	75	64
Explained Y-variance (%)	99	98	98	99
RMSEC	0.43	0.63	0.001	0.001
RMSEP	0.83	1.14	0.003	0.004
r^2 (Calibration)	0.9801	0.9859	0.9896	0.9887
r^2 (Validation)	0.9314	0.9575	0.9453	0.9483

The significance of variance is determined by full cross-validation and Martens uncertainty test and corresponds to approximately $p < 0.05$ [Negative sign (−) indicates negative significance and positive sign (+) indicates positive significance; X- indicates not been part of PLS modeling]

MicroceLac®100 at higher % RH leads to decreased material flowability. The main effects MUR constant and ΔHf had negative influence on the flowability. It means that an increase in both the moisture uptake and crystallinity (high ΔHf) leads to decreased powder flowability. The positive correlation between MUR constant, ΔHf, and CI in upper right quadrant of PC1 and PC2 is consistent with this finding. High ΔHf is associated with crystalline PBM. These materials have irregular particle shape than the relatively symmetrical spherical shaped spray-dried coprocessed excipient (Fig. 5). Thus, PBM would be expected to show poorer flowability. The high MUR constant is again associated with poorly flowing PBM and PBM-HPMC. It appears that the unprocessed hydrophilic MCC physical mixture has more water access than molecularly interacted MCC in coprocessed MicroceLac® 100. The interactions between MC and ΔHRc had positive influence on the flowability (Fig. 7a, Table II). These two parameters and MicroceLac® 100 showed high correlation in the negative side of PC1 in PCA loading and score plot. The high moisture content and high crystallization is associated with the coprocessed amorphous materials. These materials sorb more moisture and undergo crystallization. However, such materials showed better flowability than their crystalline counterpart due to their more spherical shape. This effect is also supported with SEM observations of PBM and MicroceLac®100 (Fig. 5). The SEM study showed that molecular level changes had no apparent influence on the particle shape of both unprocessed and spray dried coprocessed materials even exposure at high % RH. Thus, spray-dried coprocessed materials though undergoes high crystallization due to moisture sorption, such molecular level changes do not influence powder flowability of these materials. The interactions between MUR constant and d_{50} had positive influence on the flowability.

The CI in the PLS-1 model for PBM and MicroceLac®100 with HPMC (Fig. 7b; Table II) showed that PBM-HPMC exposed at 55% RH, and 75% RH and unexposed MicroceLac®100-HPMC and exposed at 33% RH have significant impact on the CI. The PBM-HPMC exposed at 55% RH, and 75% RH negatively influenced powder flowability. Unexposed MicroceLac®100-HPMC and exposed at 33% RH positively influenced powder flowability. The general trend of regression coefficients suggests that PBM and MicroceLac®100 containing HPMC had similar trend to PBM and MicroceLac®100 powders without HPMC exposed at different % RH. This suggests that HPMC had no influence on the powder flowability when exposed to different % RH.

The TMS PLS-1 models for PBM and MicroceLac®100 with and without HPMC are shown in Fig. 8. In these models, the magnitude and sign of the coefficient's bar indicates the impact on Y-variable or response variable such as TMS. Variables with uncertainty limits that cross the zero line are statistically insignificant variables. The positive impact on TMS indicates high TMS value, while the negative impact on TMS indicates low TMS value. A high TMS value means materials can form the stronger tablet and vice-a-versa. The TMS PLS-1 model for PBM and MicroceLac®100 without HPMC (Fig. 8a; Table II) showed that unexposed MicroceLac®100 and PBM exposed at 75% RH has respective significant positive and negative impact on the TMS. The positive correlation between TMS and unexposed MicroceLac®100 in lower left quadrant of PC1 and PC2, as well as negative correlation of PBM with TMS along PC1 is consistent with these findings (Fig. 6a and b).

This confirms the manufacturer claims that spray-drying induced amorphous content present in the coprocessed excipient enhances its compressibility due to the better plastic deformation tendency of the amorphous materials [8]. A general regression coefficients trend of MicroceLac®100 samples exposed at different % RH exhibited decrease in TMS after exposure at high % RH. The interactions between MC and MUR constant showed a negative impact on the TMS. This can be attributed to the water induced material plasticization due to presence of the excess moisture. The excess amount of water present in the powder can weaken the particle bonding strength. As a consequence, such water plasticized powders can form weaker tablets [33]. The square effect of ΔHd showed a negative impact on TMS. This is consistent with the loadings plot (Fig. 7b) where ΔHd and TMS are on opposite sides of PC2.

The TMS PLS-1 model for PBM and MicroceLac®100 with HPMC (Fig. 8b; Table II) showed that PBM-HPMC exposed at 33% RH, and 75% RH have negative impact on the TMS. In the same model, unexposed MicroceLac®100, 33% RH MicroceLac®100-HPMC, and 55% RH MicroceLac®100-HPMC showed a positive impact on TMS. A general regression coefficients trend of MicroceLac®100-HPMC samples also exhibited decrease in TMS after exposure at high % RH. The main effect of ΔHf showed a negative influence on TMS. The negative correlation of ΔHf with TMS along PC2 in the PCA loading plot corroborates this phenomenon. The ΔHf showed positive correlation with crystalline PBM along PC1. Such crystalline materials shows low plastic deformation tendency under the applied compression pressure leading to form weaker tablets [7, 34]. In contrast, ΔHRc main effect demonstrated a positive influence on TMS. This effect indicates that materials with high crystallization tendency show high TMS. This was also confirmed by the positive correlation of ΔHRc with TMS (Fig. 6a) and MicroceLac®100 along PC1 (Fig. 6b). High ΔHRc is generally associated with amorphous coprocessed materials. As mentioned earlier, amorphous material exhibits better plastic deformation, which leads to stronger tablets. In the same PLS model, interactions of ΔHRc with MUR constant displayed negative influence on the TMS. The negative correlation of ΔHRc and MUR constant with TMS along PC2 is consistent with this finding (Fig. 6b). MUR constant

is a function of material moisture uptake. This interaction implies that materials with high ΔHRc (amorphous materials) are susceptible to a small amount of added moisture. This sorbed water might reduce TMS by two mechanisms. It can induce molecular changes by promoting the crystallization of the amorphous materials [30]. This can lead to high ΔHRc. Such materials with high crystallinity form weaker tablets due to reduced plastic deformation tendency. Furthermore, sorbed water might act as plasticizer to weaken the particle bonding. The ΔHRc and d_{50} interactions also influenced TMS negatively. This means that materials with high ΔHRc and d_{50} produce weaker tablets. The negative correlation of ΔHRc and d_{50} with TMS along PC2 is consistent with this finding (Fig. 6b). It is known that large sized particles (high d_{50}) are less compactible, as they possess low specific area required for effective particle bonding. Thus, materials with large particle size may form weaker tablets [35]. Additionally, it appears that high ΔHRc was the dominant factor influencing TMS.

Sorbed water is thought to be responsible for change in ΔHRc and d_{50}. Therefore, the role of HPMC induced water sorption on the previously discussed main effects and interactions confirmed that an external addition of 5% w/w HPMC as a crystallization inhibitor appears not to protect PBM and MicroceLac® 100 from moisture sorption and associated molecular and macroscopic level changes. This might be attributed to the moisture affinity of hydrophilic HPMC [12]. Such polymer-water interaction increases overall system hygroscopicity, which can change the overall powder material properties significantly.

CONCLUSIONS

The newly developed 'DM^3' approach evaluated and quantified the relationships among critical formulation attributes (CI and TMS), storage condition (% RH), excipient (crystallization inhibitor HPMC), molecular properties (moisture sorption isotherms, MC, ΔHd, ΔHRc, ΔHf, MC, and MUR), and macroscopic properties (particle morphology and d_{50}) of a model-coprocessed excipient MicroceLac® 100. The results of statistical analyses performed by multivariate methods (MANOVA, PCA, and PLS) complimented each other. These studies showed that coprocessed MicroceLac® 100 had better formulation properties than its counterpart PBM. PBM and MicroceLac® 100 showed no change in the particle shape after exposure at high % RH in the SEM studies. However, MicroceLac® 100 showed more susceptibility to molecular level changes, specifically water induced crystallization than PBM at high % RH. The general trend of regression coefficients of PLS models of CI and TMS suggested that these formulation properties are negatively influenced at high % RH. In the same models, the main effects of the molecular properties (ΔHd, ΔHRc, ΔHf) and molecular and macroscopic interaction effects (MUR*d_{50}, MC*ΔHRc, MC*MUR, ΔHRc*MUR, ΔHRc*d_{50}) showed statistically significant impact on CI and TMS formulation parameters. Furthermore, external addition of 5% w/w HPMC as a crystallization inhibitor did not protect PBM and MicroceLac® 100 from the moisture sorption and subsequently associated molecular and macroscopic level changes. Additionally, the high susceptibility of coprocessed MicroceLac® 100 to molecular level changes that impact TMS warrant careful periodic evaluation of this material for different types of enthalpy evaluations like ΔHd, ΔHRc, and ΔHf before its actual use in formulations. Enthalpy evaluations of coprocessed MicroceLac®100 are recommended to avoid or predict the potential material changes over its shelf life.

ACKNOWLEDGMENTS

The authors gratefully acknowledge Mr. Charles Mooney from North Carolina State University, Raleigh, North Carolina for SEM analysis of PBM and MicroceLac® 100 samples. The authors are also grateful to Mr. Paul R. Johnson from Pharmaceutical Education & Research Center (PERC), Campbell University, Buies Creek, North Craolina for his help during experimentation.

REFERENCES

1. Nachaegariand SK, Bansal AK. Coprocessed excipients for solid dosage forms. Pharm Technol. 2004;28(1):52, 54, 56, 58, 60, 62, 64.
2. http://www.ipec-europe.org/UPLOADS/Mroz_PharmSciFair2009.pdf Accessed on 08/05/2014.
3. Crowley P, Martini L. Drug-excipient interactions. Pharm Technol Eur. 2001 13:26–28, 30–32, 34.
4. R. Russell. Synthetic excipients challenge all-natural organics—offer advantages/challenges to developers and formulators. Pharm Tech. 2004;38–50.
5. S.K. Nachaegariand A.K. Bansal. Co-processed excipients for solid dosage forms. Pharm Tech. 2004;52–64.
6. Block LH, Moreton RC, Apte SP, Wendt RH, Munson EJ, Creekmore JR, *et al.* Co-processed excipients. Pharmacopoeial Forum. 2009;35:1026–58.
7. G. Bolhuis, K. Kussendrager, and J. Langridge. New developments in spray-dried lactose. Pharma Tech Excip Solid Dos Forms. 2004;24–31.
8. Bolhuisand GK, Chowhan ZK. Materials for direct compression. In: Alderbornand G, Nystrom C, editors. Pharmaceutical powder compaction technology, vol. 71. New York: Marcel Dekker, Inc.; 1996. p. 419–500.
9. Hildenand LR, Morris KR. Physics of amorphous solids. J Pharm Sci. 2004;93:3–12.
10. Hancockand BC, Zografi G. Characteristics and significance of the amorphous state in pharmaceutical systems. J Pharm Sci. 1997;86:1–12.
11. http://www.fda.gov/downloads/Drugs/Guidances/ucm070305.pdf Accessed on 08/05/2014.

12. Konnoand H, Taylor L. Ability of different polymers to inhibit the crystallization of amorphous felodipine in the presence of moisture. Pharma Res. 2008;25:969–78.
13. Linand YC, Chen X. Moisture sorption–desorption–resorption characteristics and its effect on the mechanical behavior of the epoxy system. Polymer. 2005;46:11994–2003.
14. Powder Flow. United States Pharmacopoeia, USP-NF online <1174> USP 37-NF32, pp. 1052. Accessed on 07/29/2014.
15. Bulk Density and Tapped Density of Powders. United States Pharmacopoeia, USP-NF online <616> USP 37-NF32, pp. 298–300. Accessed on 07/29/2014.
16. Hu D, Haware RV, Hamad ML, Morris KR. Characterization of critical physical and mechanical properties of freeze-dried grape powder for development of a clinical patient delivery system. Pharm Dev Technol. 2013;18:146–55.
17. Crank J. The mathematics of diffusion. 2nd ed. New York: Oxford University Press; 1989.
18. Tablet Breaking Force. United States Pharmacopoeia, USP-NF online <1217> USP 37-NF32, pp. 1146–1148. Accessed on 07/29/2014.
19. Martensand H, Martens M. Modified Jack-knife estimation of parameter uncertainty in bilinear modelling by partial least squares regression (PLSR). Food Qual Prefer. 2000;11:5–16.
20. http://www.pqri.org/blenduniformity/imagespdfs/FDADraftGuide.pdf Accessed on 07/30/14.
21. Swaminathanand V, Kildsig D. An examination of the moisture sorption characteristics of commercial magnesium stearate. AAPS PharmSciTech. 2001;2:73–9.
22. Mangel A. Investigating a range of solid samples by automatic water sorption. J Therm Anal Calorim. 1999;55:581–99.
23. Airaksinen S, Karjalainen M, Shevchenko A, Westermarck S, Leppänen E, Rantanen J, *et al.* Role of water in the physical stability of solid dosage formulations. J Pharm Sci. 2005;94:2147–65.
24. Sing KSW, Haul RAW, Pierotti RA, Siemieniewska T. Reporting physisorption data for gas/solid systems with special reference to the determination of surface area and porosity (Recommendations 1984). Pure Appl Chem. 1985;57:603–19.
25. Meggle anhydrous lactose grade for direct compression:DuraLac® H.
26. Figura LO. The physical modification of lactose and its thermoanalytical identification. Thermochim Acta. 1993;222:187–94.
27. Listiohadi Y, Hourigan J, Sleigh R, Steele R. Thermal analysis of amorphous lactose and α-lactose monohydrate. Dairy Sci Technol. 2009;89:43–67.
28. Ticehurst MD, York P, Rowe RC, Dwivedi SK. Characterisation of the surface properties of α-lactose monohydrate with inverse gas chromatography, used to detect batch variation. Int J Pharm. 1996;141:93–9.
29. GombÁs Á, Szabó-Révész P, Kata M, Regdon Jr G, Erős I. Quantitative determination of crystallinity of α-lactose monohydrate by DSC. J Therm Anal Calorim. 2002;68:503–10.
30. Shalaevand EY, Zografi G. How does residual water affect the solid-state degradation of drugs in the amorphous state? J Pharmacol Sci. 1996;85:1137–41.
31. Haware RV, Tho I, Bauer-Brandl A. Application of multivariate methods to compression behavior evaluation of directly compressible materials. Eur J Pharm Biopharm. 2009;72:148–55.
32. Haware RV, Shivagari R, Johnson PR, Staton S, Stagner WC, Gupta MR. Application of multivariate methods to evaluate the functionality of bovine- and vegetable-derived magnesium stearate. J Pharm Sci. 2014;103:1466–77.
33. Chamarthy SP, Diringer FX, Pinal R. The Plasticization-Antiplasticization Threshold of Water in Microcrystalline Cellulose: A Perspective Based on Bulk Free Volume. Water Properties in Food, Health, Pharmaceutical and Biological Systems: ISOPOW 10, Wiley-Blackwell; 2010. pp. 297–314.
34. Felland JT, Newton JM. The tensile strength of lactose tablets. J Pharm Pharmacol. 1968;20:657–9.
35. Nystromand C, Karehill P. The importance of intermolecular bonding forces and the concept of bonding surface area. In: Alderbornand G, Nystrom C, editors. Pharmaceutical powder compaction technology, vol. 71. New York: Marcel Dekker, Inc.; 1996. p. 17–53.